TRI-PORT CONVERTER FOR FLEXIBLE ENERGY CONTROL OF PV-FED EV WITH SRM

[1]A. D. Waghmode, [2]Dr. M. G. Poddar,
[1]Student, 2Associate Professor,
[1]Post Graduation (Control System),
[1]MBE's college of engineering, Ambajogai,India

ABSTRACT

Automotive companies are developing electric, hybrid electric vehicles because there is the requirements for reducing emissions and improving fuel economy. Electric vehicles (EVs) can reduce greenhouse gas emissions while switched reluctance motor (SRM) is one of the promising motor for such applications. Switched reluctance motors (SRMs) have low cost, ease of manufacturing, and robustness in withstanding centrifugal force advantages. Therefore, they are very suitable for high-speed applications. In order to extend the EVs' driving miles, photovoltaic (PV) panels are used on the vehicle helps to decrease the reliance on vehicle batteries. Six operating modes are presented, in which four of which are developed for driving and two for standstill onboard charging. Simulation results are based on MATLAB/Simulink and experiments prove the effectiveness of the proposed tri-port converter, which have potential economic implications to improve the market acceptance of EVs.

Index Terms—Electric vehicles (EVs), photovoltaic's (PVs), switched reluctance motors (SRMs).

I. INTRODUCTION

An electric vehicle is also called an EV, uses one or more electric motors or traction motors for propulsion. The increasing popularity of electric vehicles (EVs) is attributed to the savings in fuel costs compared to conventional internal combustion engine (ICE) vehicles. Electric vehicles (EVs) provide a feasible solution to reduce greenhouse gas emissions and thus become a hot topic for research and development [1]-[4].In order to extend the EVs driving miles a photovoltaic (PV) panels are used and for providing motor drive switched reluctance motor (SRM) is used. Now a days there is restriction on wide application of EVs because of current battery technologies [5]-[7]. An axial to axial flux compound structure permanent-magnet synchronous machine (CS-PMSM) system is used for hybrid electric vehicles (HEVs) that are enables the internal combustion engine (ICE) to operate at optimum efficiency region independent of road conditions because of that the fuel consumption and emissions is decreased also the wide use of high performance permanent magnet machines are used because of that limitations are occurred on wide application of EVs [8],[9] .In order to overcome these issues, a photovoltaic (PV) panel and a switched reluctance motor (SRM) are introduced to provide power supply and motor drive, respectively. First, by adding the PV panel on top of the EV, a sustainable energy source is achieved. Now a days ,a typical passenger car has a surface enough to install a 250-W PV panel [10]. Second, a SRM needs no rare-earth Permanent Magnets and is also robust so that it receives increasing attention in EV applications [11]-[16] . While PV panels having low-power density for traction drives, they can be used to charge batteries most of time. Generally, the PV-fed EV has a similar structure to the hybrid electrical vehicle (HEV), whose internal combustion engine (ICE) is replaced by the PV panel. The Fig.1. shows the PV-fed EV system . Its key components include an off-board charging station, batteries, PV, and power converters [17]-[19].Redesign the motor to include some onboard charging function in order to decrease the energy conversion processes [20].For vehicles using grid power to charge the battery are not engaged during the charging time, so there is a possibility to use them in the charger circuit to have an onboard integrated charger. A 20-kw split-phase PM motor for EV charging is used .The on-board charger gives flexibility to charge anywhere where there is an electric power outlet available. However, the on-board type has the drawback of adding weight, cost to the vehicle and volume . The paper proposed a modular structure of driving topology .Based on the intelligent power modules(IPMs),a four-phase half bridge converter is employed to achieve grid-charging and driving .Although modularization supports mass production, the use of half or full bridge topology reduces the system reliability (e.g., shoot-through issues). For grid-charging, the grid should be connected to the generator rectifier because of that the energy conversion process is increased and the charging efficiency is decreased. The control strategy and an effective topology for PV-fed EVs is not yet developed. Because the PV has different characteristics to ICEs, solar energy utilization and the

maximum power point tracking (MPPT) are the unique factors for the PV-fed EVs. In order to achieve low-cost and flexible energy flow modes, a low-cost tri-port converter is proposed in this paper to coordinate the SRM, PV panel, and battery.

II. TOPOLOGY AND OPERATIONAL MODES

A. Proposed Topology and Working Modes

The PV, battery, and SRM these are three energy terminal of the given proposed tri-port topology . They are linked by a power converter that consists of four switching devices (S0 −S3), four diodes (D0 −D3), and two relays, as shown in Fig. 2. By controlling relays J1 and J2, the six operation modes of the proposed tri-port topology are supported , as shown in Fig. 3.And these relay actions are illustrated in Table I. In mode 1, PV is the energy source to drive the SRM and that time battery is chraged . In mode 2, the battery and PV are both the energy sources to drive the SRM. In mode 3, the PV is the driving source and the battery is idle. In mode 4, the battery is the driving source and the PV is in idle condition . In mode 5, the battery is charged by a single-phase grid while both the SRM and PV are idle. In mode 6, the battery is charged by the PV and the SRM is idle in condition.

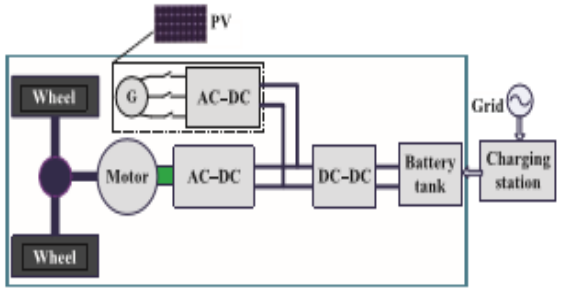

Fig.1.PV-fed HEV

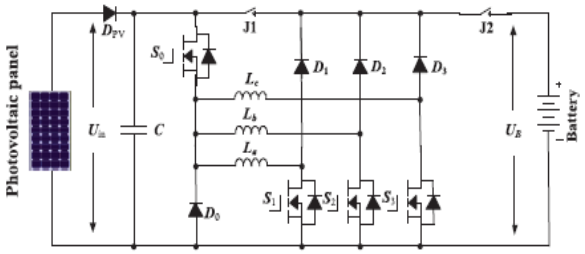

Fig. 2. Proposed tri-port topology for PV-powered SRM drive.

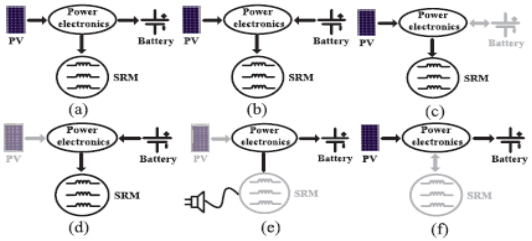

Fig. 3. Six operation modes of the proposed tri-port topology. (a) Mode 1. (b) Mode 2. (c) Mode 3. (d) Mode 4. (e) Mode 5. (f) Mode 6.

Table I J1 and J2 actions under different modes

Mode	J1 and J2
1	J1 turn-off; J2 turn-on
2	J1 and J2 turn-on
3	J1 turn-on; J2 turn-off
4	J1 and J2 turn-on
5	J1 and J2 turn-on
6	J1 turn-off; J2 turn-on

B. Driving Modes

To provide traction drive to the vehicle ,the operating modes 1 to 4 i.e. driving modes are used.

1) Mode 1: The energy generated from the PV panel is more than the SRM needed at the light loads of operation that time the system operates in mode 1.Fig. 4(a) shows the corresponding operation circuit , in which relay J1 turns off and relay J2 turns on. The PV panel energy feeds the energy to SRM and charges the battery; so in this mode, the battery is charged in EV operation condition.

2) Mode 2: Both the PV panel and battery supply power to the SRM, when the SRM operates in heavy load such as uphill driving or acceleration . Fig. 4(b) shows the corresponding operation circuit in which relay J1 and J2 are turned on.

3) Mode 3: The PV panel is the only energy source to drive the vehicle that time the battery is out of power. The corresponding operation circuit is shown in Fig. 4(c),in which J1 turns on and J2 turns off.

4) Mode 4: Due to low solar irradiation, the PV cannot generate electricity the battery supplies power to the SRM. The corresponding topology is illustrated in Fig. 4(d). In this mode, relay J1 and J2 both are conducting.

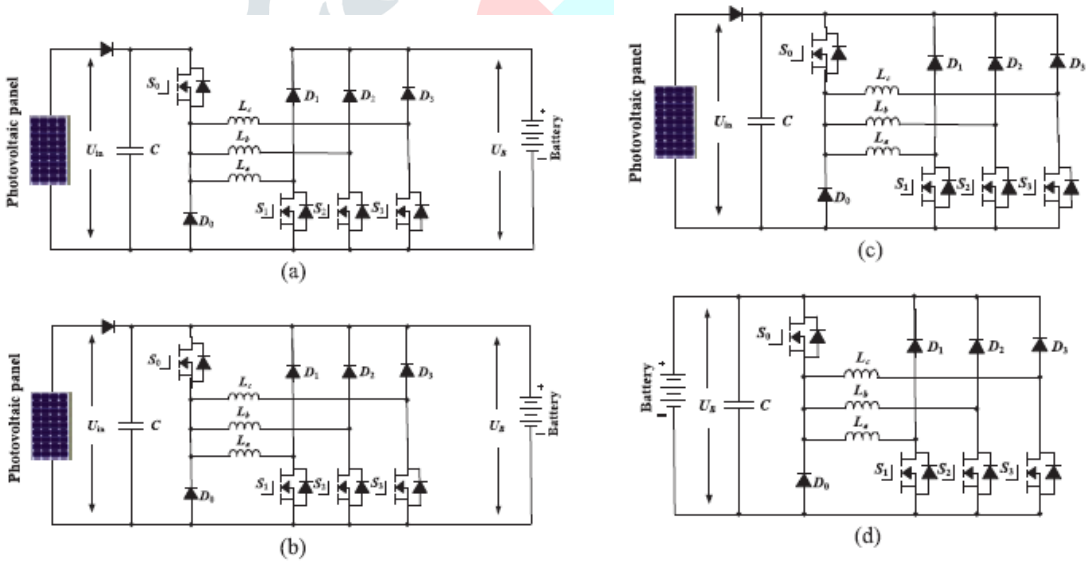

Fig. 4. Equivalent circuits under driving modes. (a) Operation circuit under mode 1. (b) Operation circuit under mode 2. (c) Operation circuit under mode 3. (d) Operation circuit under mode 4.

C. Battery Charging Modes

The battery charging modes are operating modes 5 and 6.

5) Mode 5: An external power source is needed to charge the battery, such as ac grid, when PV cannot generate electricity. The corresponding circuit is shown in Fig. 5(a). J1 and J2 both relay are turn on. Without changing the motor structure , point A is central tapped of phase windings that can be easily achieved. One of the three-phase windings is split and its midpoint is pulled out, as shown in Fig. 5(a). La1 and La2 are the phase winding which are employed as input filter inductors. For grid charging these inductors are used as a part of the drive circuit to form an ac–dc rectifier .

6) Mode 6: When the EV is parked under the sun, the PV panel can charge the battery .The corresponding charging circuit is shown in Fig. 5(b),when J1 turns off and J2 turns on.

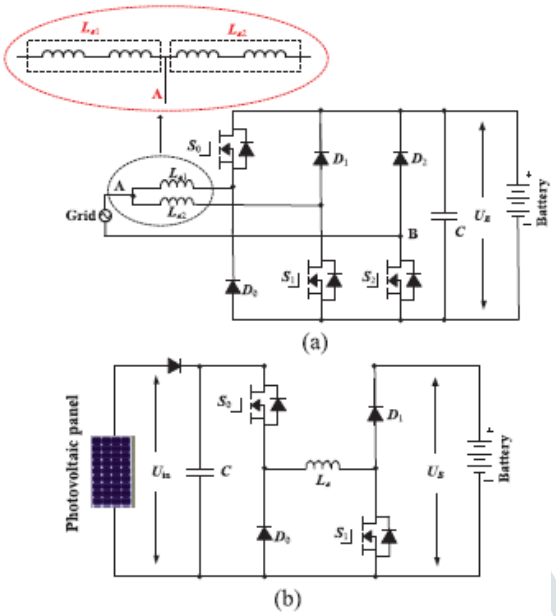

Fig. 5. Equivalent circuits of charging condition modes. (a) Grid charging mode. (b) PV source charging mode.

III. CONTROL STRATEGY UNDER DIFFERENT MODES

A control strategy under different modes is designed, in order to make the best use of solar energy for driving the EV.

A. Single Source Driving Mode

There are three types of driving i.e. PV-driving, battery-driving, and PV and battery parallel fed source, according to the difference in the power sources . Mode 2 can be adopted to support enough energy and make full use of solar energy, when PV power cannot support the EV in a heavy load condition. Fig. 6(a) shows the equivalent power source; the corresponding PV panel working points are illustrated in Fig.6(b).Because the PV panel is paralleled with the battery, the PV panel voltage is clamped to the battery voltage UB. In mode 2, there are three working states which are winding excitation, energy recycling, and freewheeling states, as shown in Fig. 7. Modes 3 and 4 have similar working states to mode 2 ,only the difference is that the PV is the only source in mode 3 while the battery is the only source in mode 4.

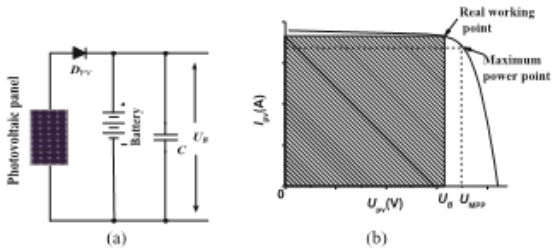

Fig.6. Power supply at mode 2. (a) Compound power source . (b)Working point of the PV.

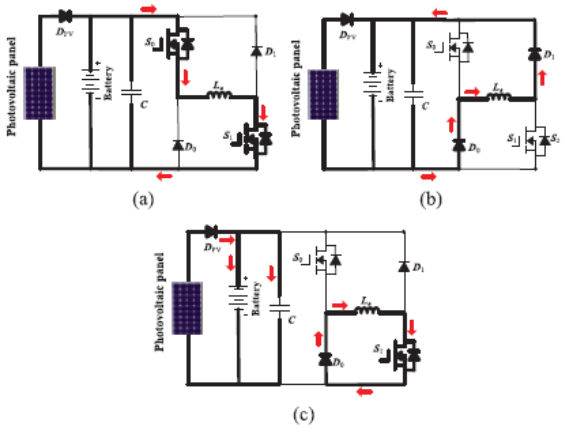

Fig. 7. Working states at mode 2. (a) Winding excitation state. (b)recycling state. (c) Freewheeling state.

Neglecting the voltage drop across the diodes and power switches , the phase voltage is given by,

$$U_{in} = R_k\, i_k + \frac{d\psi(i_k,\theta_r)}{dt}$$

$$U_{in} = R_k i_k + L_k \frac{di_k}{dt} + i_k \omega_r \frac{dL_k}{d\theta_r} \quad (1)$$

Where, Uin is the dc-link voltage, k is phases a, b, or c, ik is the phase current, Lk is the phase inductance, Rk is the phase resistance, ϑr is the rotor position, ψ(ik,ϑr) is the phase flux linkage depending on the rotor position and phase current , and ωr is the angular speed. The third term in (1) is the back EMF voltage which is given by,

$$e_k = i_k \omega_r + \frac{dL_k}{d\theta_r} \quad (2)$$

Hence, the phase voltage is found by,

$$U_k = R_k i_k + L_k \frac{di_k}{dt} + e_k \quad (3)$$

In the excitation region when S0 and S1both are ON, it will induce a current in phase a winding, as shown in Fig. 7(a). Phase a winding is subjected to the positive dc bus voltage,

$$+U_{in} = R_k i_k + L_k \frac{di_k}{dt} + e_k \quad (4)$$

The phase current is in a freewheeling state in a zero-voltage loop, when S0 is OFF and S1 is ON, as shown in Fig. 7(c), the phase voltage is zero,

$$0 = R_k i_k + L_k \frac{di_k}{dt} + e_k \quad (5)$$

In the demagnetization region, S0 and S1 are both OFF, and the phase current will flow back to the power supply, as shown in Fig. 7(b). In this state, the phase winding is subjected to the negative dc bus voltage, and the phase voltage is,

$$-U_{in} = R_k i_k + L_k \frac{di_k}{dt} + e_k \quad (6)$$

In single-source driving mode, the voltage-PWM control is employed as the basic scheme, as illustrated in Fig. 8. According to the given speed ω∗, the voltage-PWM control is activated at speed control.

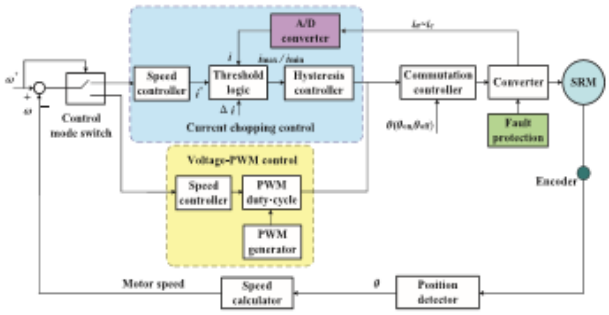

Fig. 8.SRM control strategy under single-source driving mode.

B.Driving-Charging Hybrid Control Strategy

In the driving-charging hybrid control, the PV panel is the driving source and the battery is charged by the freewheeling current, as illustrated in drive mode 1. There are two control objectives these are MPPT of the PV panel and speed control of the SRM. In this the dual-source condition is switched from a PV-driving mode. First, the motor speed is controlled at a given speed in mode 3 and then, J2 is turned on and J1 is turned off to switch to mode 1.For tracking maximum power of PV panel ,the turn -off angle is controlled There are three steady working states are given for the dual-source mode (mode 1), as shown in Fig. 9.

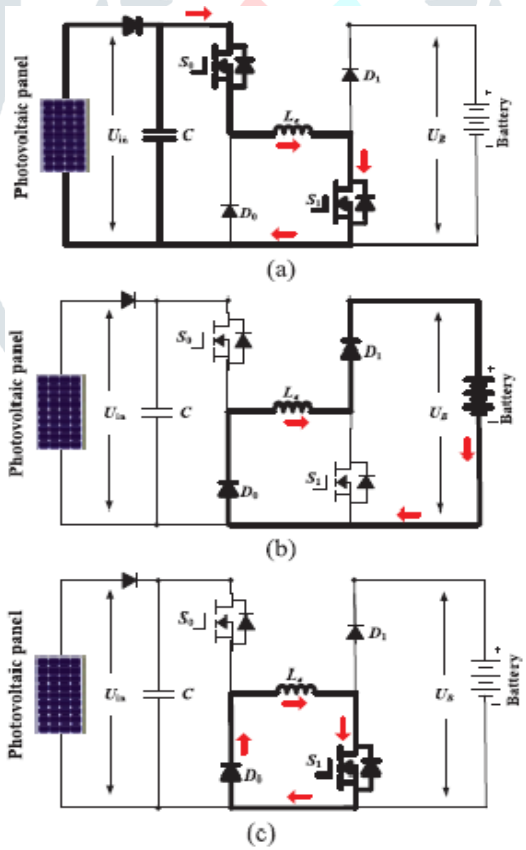

Fig. 9. Mode 1 working states. (a) Winding exciting state. (b) Battery charging state. (c) Freewheeling state.

In Fig. 9(a), S0 and S1 both are conducting, the PV panel charges the SRM winding to drive the motor ,this is the winding excitation state. In Fig. 9(b), S0 and S1 turn-off; and the battery is charged with freewheeling current of the phase winding ,this is the battery charging state. In Fig. 9(c), the S0 is turn-off and S1 is turn-on shows a freewheeling state.

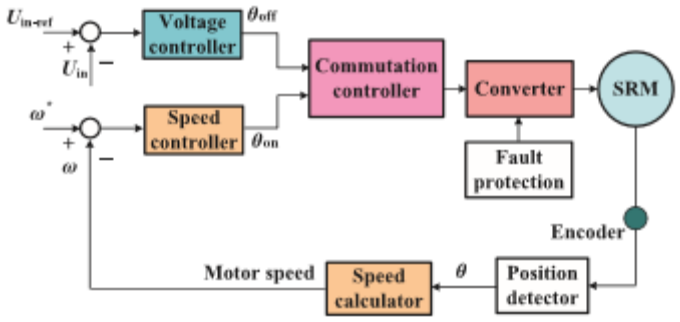

Fig.10.Control strategy under driving-charging mode(mode 1)

Fig. 10 shows the control strategy under driving-charging mode. In Fig. 10, ϑon is the turn-on angle and ϑoff is the turn-off angle of SRM. The speed of SRM can be controlled , by adjusting turn-on angle. And by adjusting turn-off angle, the MPPT of PV panel can be achieved .The turn-off angle can control the charging current to the battery.

C.Grid-Charging Control Strategy

In single-phase grid charging, there are four basic charging states in which S0 is always turned off. When the grid instantaneous voltage is greater than zero, the two working states are presented in Fig. 11(a) and (b). In Fig. 11(a), S1 and S2 conduct, the phase winding La2 is charged by grid voltage, the corresponding equation can be expressed as (7).In Fig. 11(b), S1 turns off and S2 turns on , the grid is connected in series with phase winding to charges the battery, the corresponding equation can be expressed as (8)

$$U_{grid} = L_{a2} \cdot \frac{di_{grid}}{dt} \quad (7)$$

$$U_B - U_{grid} = L_{a2} \cdot \frac{di_{grid}}{dt} \quad (8)$$

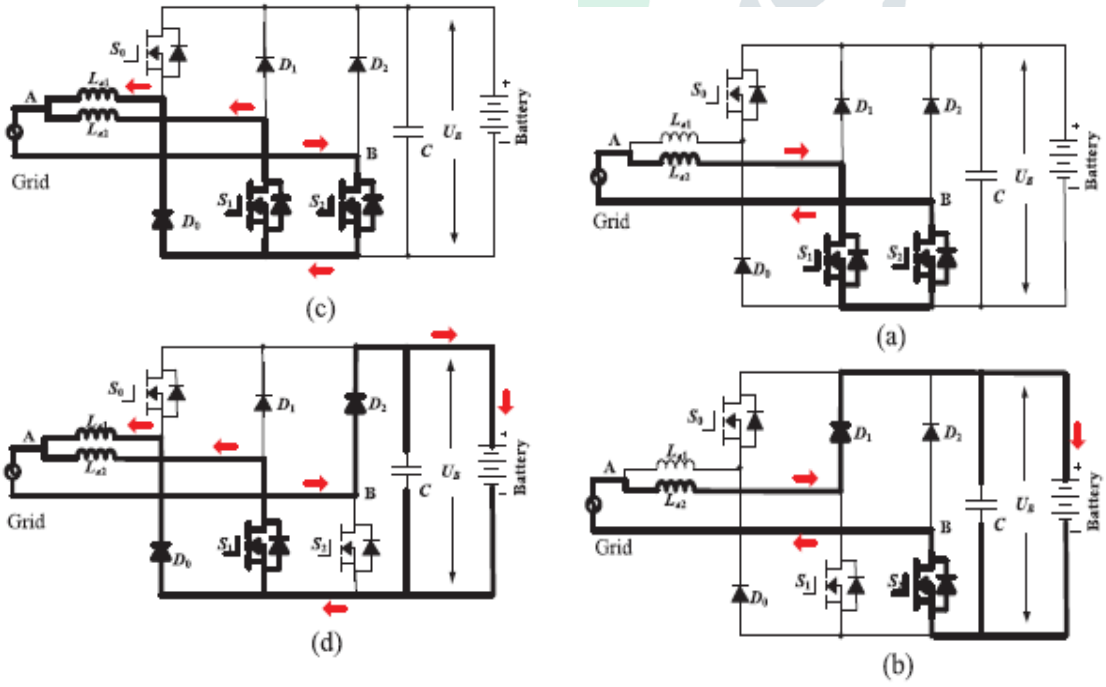

Fig. 11. Mode 5 charging states. (a) Grid charging state 1 (Ugrid > 0). (b) Grid charging state 2 (Ugrid > 0). (c) Grid charging state 3 (Ugrid < 0). (d) Grid charging state 4 (Ugrid < 0).

When the grid instantaneous voltage is below zero, the two working states are presented in Fig. 11(c) and (d). In Fig. 11(c), S1 and S2 both are conducting, the grid voltage charges the phase winding La1 and La2, the corresponding equation can be expressed as (9).In Fig. 11(d), S1 keeps conducing and S2 turns off, the grid is connected in series with phase winding La1 and La2 to charges the battery, the corresponding equation can be expressed as (10)

$$U_{grid} = \frac{L_{a1} + L_{a2}}{L_{a1} \cdot L_{a2}} \cdot \frac{di_{grid}}{dt} \qquad (9)$$

$$-U_B - U_{grid} = \frac{L_{a1} + L_{a2}}{L_{a1} \cdot L_{a2}} \cdot \frac{di_{grid}}{dt} \qquad (10)$$

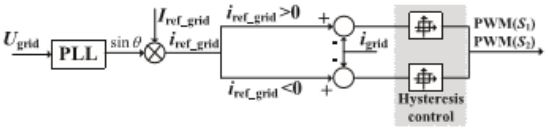

Fig. 12. Grid-connected charging control (mode 5).

In Fig. 12, Ugrid is the grid voltage ; in which the phase information can be got; by the phase lock loop (PLL) .Iref _ grid is the given amplitude of the grid current. The instantaneous grid current reference iref_grid can be calculated by combining sin9 and Iref_grid. In this mode, when Ugrid > 0, the inductance is given as La2; when Ugrid < 0, the inductance is paralleled La1 and La2; in order to take the change in the inductance, hysteresis control is employed to realize grid current regulation. Further more ,hysteresis control has excellent loop performance, global stability, and small phase lag that make grid-connected control stable.

D.PV-Fed Charging Control Strategy

In this mode, the PV charges the battery directly by the driving topology. The phase windings are employed as inductor, and the driving topology can be functioned as interleaved buck– boost charging topology. For one phase, there are two states which are as shown in Fig. 13(a) and (b) i.e. phase inductance charging and battery charging respectively. When S0 and S1 both are turn on, the PV panel charges phase inductance; when S0 and S1 both are turn off, the phase inductance discharges energy to battery. According to the state-of-charging (SoC), there are three stages are used to make full use of solar energy and maintain battery in healthy condition, as illustrated in Fig. 13(c) i.e. charging control strategy. During stage 1, the corresponding battery SoC is in SoC0−SoC1, the battery is in extremely lack energy condition, the MPPT control strategy is employed to make full use of solar energy, in which current of PV panel and voltage of input are compared at MPPT,we get the voltage of PV –ref .This voltage is given to the PID controller and at the last PWM generator gives the output PWM (S0) and PWM(S1).During stage 2, the corresponding battery SoC is in SoC1−SoC2,the constant-voltage control is adopted to charge the battery, in which S-R flip flop is used. During stage 3, the corresponding battery SoC is in SoC2−100%,the micro-current charging is adopted. In order to simplify the control strategy, the constant voltage is employed in PV panel MPPT control.

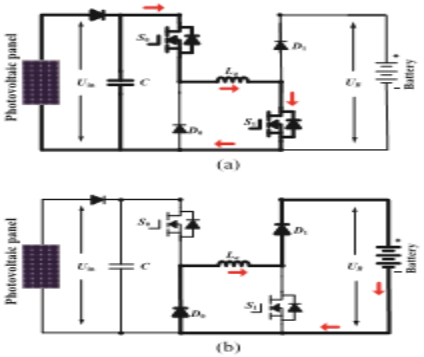

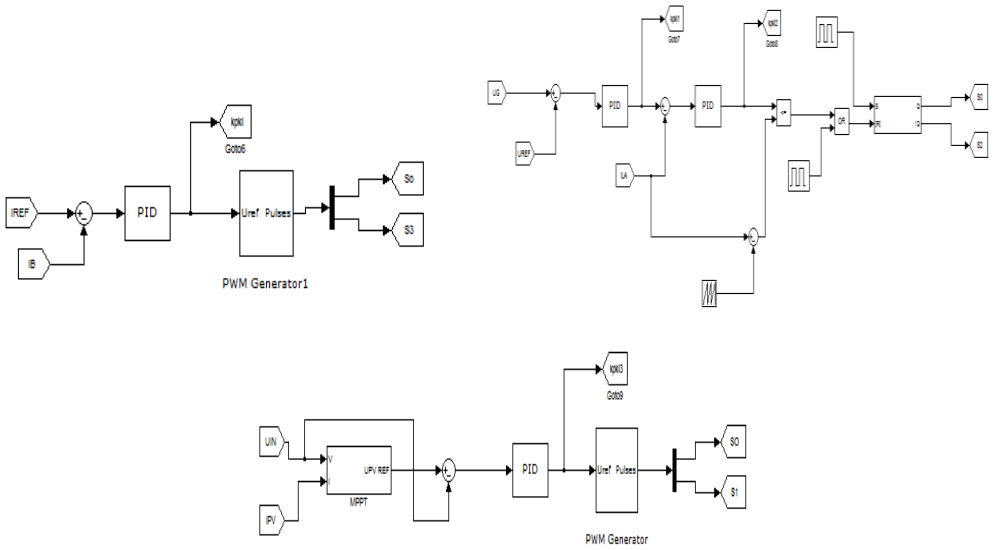

Fig. 13. Mode 6 charging states and control strategy.(iii) Charging control strategy in stage 1.

IV. SIMULATION

A 12/8 SRM is first modeled in MATLAB/Simulink using parameters in Table II. Fig.14(a)presents the simulation results atmode1.The load torque is set as 35 Nm ,the PV panel voltage is controlled at the MPP. The freewheeling current is used to charge the battery. Fig. 14(b) shows the simulation results of the single-source driving modes (modes 2–4). Fig. 15 shows the simulation results of charging where Fig. 15(a) is for grid-charging. The positive half current quality is better than the negative half that is caused by the change in the grid-connected inductance. Fig. 15(b) and (c) is for PV-charging. Fig. 15(b) presents the step change from stage 1 to 2. In stage 1, the battery is low in SoC. In order to achieve MPPT of the PV, the constant-voltage control is employed and the PV output voltage is controlled at MPP (310 V), as shown in Fig. 15(b). In stage 2, a constantvoltage is adopted; the reference voltage is set to 355 V. As shown in Fig. 15(b), the charging converter output voltage is controlled at reference voltage in the step change from stage 1 to 2. In stage 3, 1-A trickle charging is also achieved, as shown in Fig. 15(c).

Table II Simulation Parameter

Parameter	Value
SRM	12/8
PV panel Maximum power point voltage reference voltage	310 V
Battery voltage	350 V
Constant voltage control reference voltage	355 V
Constant current control reference current	1 A
Mode 1, charging current	60 A
Mode 4, driving speed	1250 r/min
Mode 6, constant voltage charging reference	355 V
Mode 6, constant current charging reference	1 A

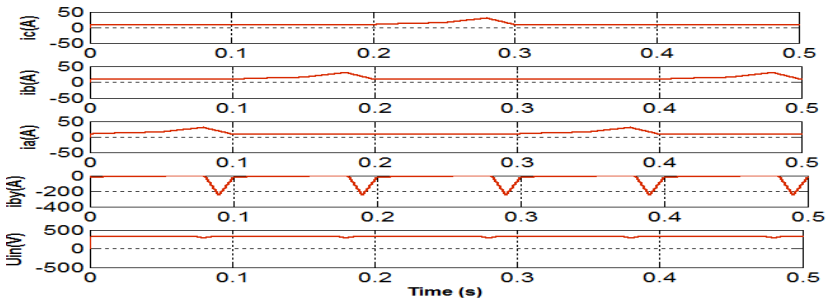

(a)

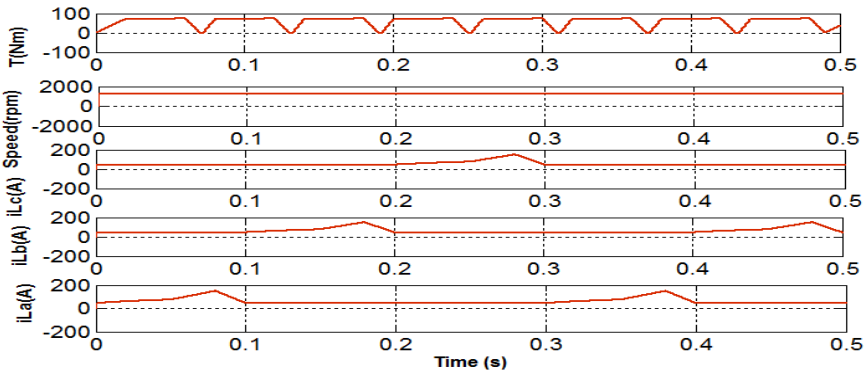

(b)

Fig. 14. Simulation results for driving conditions at modes 1, 3, and 4. (a) Simulation results of driving-charging mode (mode 1). (b) Simulation results of single-source driving mode (modes 3 and 4).

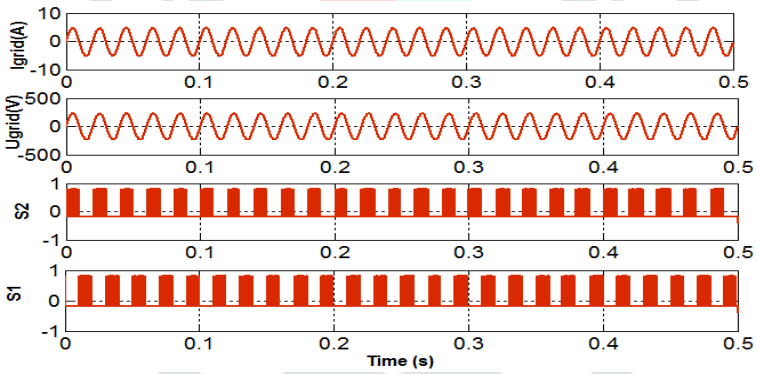

(a)

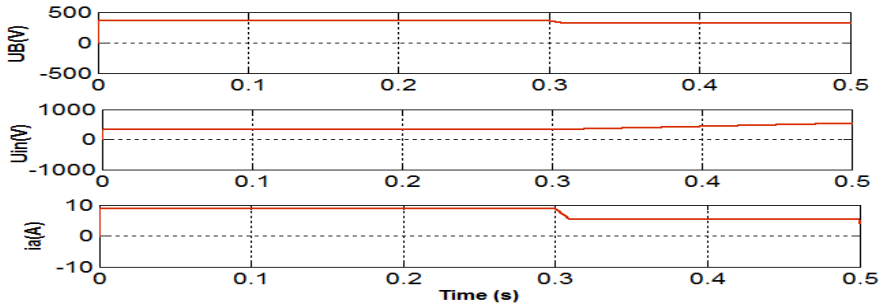

(b)

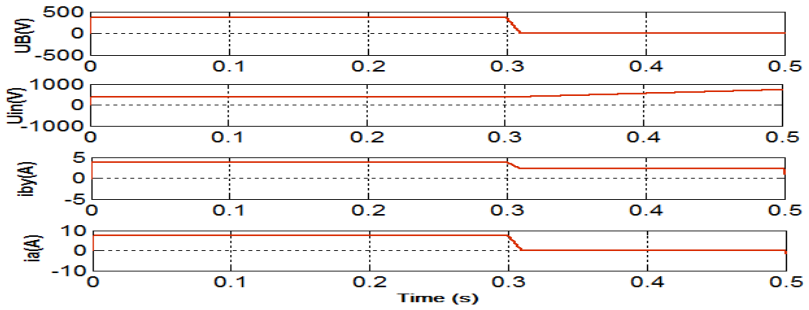

(c)

Fig. 15. Simulation results for charging modes. (a) Grid charging (mode 5). (b) PV charging mode 6 (stages 1–2). (c) PV charging mode 6 (stages 2–3).

V. CONCLUSION

In order to tackle the range anxiety of using EVs and decrease the system cost, a combination of the PV panel and SRM is proposed as the EV driving system. The main contributions of this paper are as follows.

1)The efficiency of the system is increased due to PID controller.

2)The PV panel, battery, and SRM is coordinated by a tri-port converter.

3) In this ,six working modes are developed to achieve flexible energy flow for driving control, driving/charging hybrid control, and charging control.

4) A grid-charging topology is formed without a need for external power electronics devices.

5) A PV-fed battery charging control scheme is developed to improve the solar energy utilization.

Since PV-fed EVs are a greener and more sustainable technology than conventional ICE vehicles, this work will easily provide a feasible solution to reduce the total costs and CO2 emissions of electrified vehicles. Furthermore, the proposed technology may also be applied to similar applications such as fuel cell powered EVs. Fuel cells have a much high-power density and are thus better suited for EV applications.

REFERENCES

[1] **A. Emadi, L. Young-Joo, and K. Rajashekara, "Power electronics and motor drives in electric, hybrid electric, and plug-in hybrid electric vehicles," IEEE Trans. Ind. Electron., vol. 55, no. 6, pp. 2237–2245, Jun. 2008.**

[2] L. K. Bose, "Global energy scenario and impact of power electronics in 21st century," IEEE Trans. Ind. Electron., vol. 60, no. 7, pp. 2638–2651, Jul. 2013.

[3] J. De Santiago et al., "Electrical motor drivelines in commercial all electric vehicles: A review," IEEE Trans. Veh. Technol., vol. 61, no. 2, pp. 475–484, Feb. 2012.

[4] Z. Amjadi and S. S. Williamson, "Power-electronics-based solutions for plug-in hybrid electric vehicle energy storage and management systems," IEEE Trans. Ind. Electron., vol. 57, no. 2, pp. 608–616, Feb. 2010.

[5]A.Kuperman,U.Levy, J.Goren,A.Zafransky,andA.Savernin,"Battery charger for electric vehicle traction battery switch station," IEEE Trans. Ind. Electron., vol. 60, no. 12, pp. 5391–5399, Dec. 2013.

[6] S.G.Li,S.M.Sharkh,F.C.Walsh,andC.N.Zhang,"Energy and battery management of a plug-in series hybrid electric vehicle using fuzzy logic," IEEE Trans. Veh. Technol., vol. 60, no. 8, pp. 3571–3585, Oct. 2011.

[7] H. Kim, M. Y. Kim, and G. W. Moon, "A modularized charge equalizer using a battery monitoring IC for series-connected Li-ion battery strings in electric vehicles," IEEE Trans. Power Electron., vol. 28, no. 8, pp. 3779–3787, May 2013.

[8] Z. Ping, Z. Jing, L. Ranran, T. Chengde, and W. Qian, "Magnetic characteristics investigation of an axial–axial flux compound-structure PMSM used for HEVs," IEEE Trans. Magn., vol. 46, no. 6, pp. 2191–2194, Jun. 2010.

[9] A. Kolli, O. Béthoux, A. De Bernardinis, E. Labouré, and G. Coquery, "Space-vector PWM control synthesis for an H-bridge drive in electric vehicles," IEEE Trans. Veh. Technol., vol. 62, no. 6, pp. 2441–2452, Jul. 2013.

[10] Y. Hu, C. Gan, W. Cao, W. Li, and S. Finney, "Central-tapped node linkedmodularfaulttolerancetopologyforSRMbasedEV/HEVapplications," IEEE Trans. Power Electron., vol. 31, no. 2, pp. 1541–1554, Feb. 2016.

[11] S. M. Yang and J. Y. Chen, "Controlled dynamic braking for switched reluctance motor drives with a rectifier front end," IEEE Trans. Ind. Electron., vol. 60, no. 11, pp. 4913–4919, Nov. 2013.

[12] B. Bilgin, A. Emadi, and M. Krishnamurthy, "Comprehensive evaluation of the dynamic performance of a 6/10 SRM for traction application in PHEVs," IEEE Trans. Ind. Electron., vol. 60, no. 7, pp. 2564–2575, Jul. 2013.

[13] M. Takeno, A. Chiba, N. Hoshi, S. Ogasawara, M. Takemoto, and M. A. Rahman, "Test results and torque improvement of the 50-kW switched reluctance motor designed for hybrid electric vehicles," IEEE Trans. Ind. Appl., vol. 48, no. 4, pp. 1327–1334, Jul./Aug. 2012.

[14] A. Chiba, M. Takeno, N. Hoshi, M. Takemoto, S. Ogasawara, and M. A. Rahman, "Consideration of number of series turnsin switchedreluctancetractionmotorcompetitivetoHEVIPMSM,"IEEETrans.Ind. Appl., vol. 48, no. 6, pp. 2333–2340, Nov./Dec. 2012.

[15] I. Boldea, L. N. Tutelea, L. Parsa, and D. Dorrell, "Automotive electric propulsion systems with reduced or no permanent magnets: An overview," IEEE Trans. Ind. Electron., vol. 60, no. 9, pp. 5696–5710, Oct. 2014.

[16] X.D.Xue,K.W.E.Cheng,T.W.Ng,andN.C.Cheung,"Multi-objective optimization design of in-wheel switched reluctance motors in electric vehicles," IEEE Trans. Ind. Electron., vol. 57, no. 9, pp. 2980–2987, Sep. 2010.

[17] Y. J. Lee, A. Khaligh, and A. Emadi, "Advanced integrated bidirectional AC/DC and DC/DC converter for plug-in hybrid electric vehicles," IEEE Trans. Veh. Technol., vol. 58, no. 8, pp. 3970–3980, Oct. 2009.

[18] M. Yilmaz and P. T. Krein, "Review of battery charger topologies, charging power levels, and infrastructure for plug-in electric and hybrid vehicles," IEEE Trans. Power Electron., vol. 28, no. 5, pp. 2151–2169, May 2013.

[19] A. Khaligh and S. Dusmez, "Comprehensive topological analysis of conductive and inductive charging solutions for plug-in electric vehicles," IEEE Trans. Veh. Technol., vol. 61, no. 8, pp. 3475–3489, Oct. 2012.

[20] S. Haghbin, S. Lundmark, M. Alakula, and O. Carlson, "Grid-connected integrated battery chargers in vehicle applications: Review and new solution," IEEE Trans. Ind. Electron., vol. 60, no. 2, pp. 459–473, Feb. 2013.